

Electrospinning Fabrication and Characterization of Poly(vinyl alcohol)/Layered Double Hydroxides Composite Fibers

Qing Qin, Ya Liu, Si-Chong Chen, Fei-Yu Zhai, Xin-Ke Jing, Yu Zhong Wang

Center for Degradable and FR Polymeric Materials, National Engineering Laboratory of Eco-Friendly Polymeric Materials (Sichuan), College of Chemistry, Sichuan University, Chengdu, 610064, P.R. China

Received 25 April 2011; accepted 23 January 2012

DOI 10.1002/app.36876

Published online in Wiley Online Library (wileyonlinelibrary.com).

ABSTRACT: Nanofibers of poly(vinyl alcohol) (PVA)/layered double hydroxide (Mg-Al LDH) composites are prepared by the electrostatic fiber spinning using water as the solvent at a high voltage of 21 kV. Either inorganic LDH carbonate (LDH-CO₃) or L-lactic acid-modified LDH (Lact-LDH) is used for incorporating with PVA. Scanning electron microscopy SEM investigations on the nanofibers suggest that the average diameters of PVA/LDH composite fibers are smaller than that of neat PVA. Transmission electron microscopy (TEM) investigations indicate that the dispersity of the LDH in PVA matrix is much improved after modification with L-lactic acid. The mechanical prop-

erties of the PVA/LDH fibers are obviously enhanced compared to that of neat PVA. For example, the tensile stress and elongation at break of the PVA/Lact-LDH electrospun fibrous mat with 5 wt % Lact-LDH are 31.7 MPa and 36.7%, respectively, which are significantly higher than those of neat PVA, and also higher than those of PVA/LDH-CO₃ owing to the better dispersity of Lact-LDH nanoparticles. © 2012 Wiley Periodicals, Inc. *J Appl Polym Sci* 000: 000–000, 2012

Key words: electrospinning; nanofibers; mechanical properties; nanocomposites; dispersions

INTRODUCTION

In recent years, polymer fibers especially the nanoscale has aroused considerable technological interest owing to their high surface area, multiple surface functionalities, variations in the wetting behavior, and higher effective porosity, and so on.¹ Traditional methods of polymer fiber production such as melt spinning, solution spinning, and gel state spinning only produce can fibers with an average diameter range of 5–500 μm.¹ The electrospinning was firstly explored in 1934 as a simple and low-cost approach to produce nonwoven membranes of nanofibers.^{2–6} The electrospinning method relies on electrostatic force to produce fibers by extruding continuous strand of polymer solutions or melts. When the electrostatic force is higher than the surface tension of the solution, a charged jet of fluid is produced. As the solvent evaporates or the melt solidifies, the fibers are collected on a grounded collector as a nonwoven mat. These fibrous mats show extremely large specific surface area, wide ranging porosity,

and excellent flexibility. Owing to these interesting properties, this technique has attracted extensive attention recently for a wide variety of applications, including ultra filtration, wound-dressing materials, composite-fiber materials, tissue scaffold, and so on.^{7–11}

Recently, there are several investigations for electrospinning of biodegradable polymers because they are widely applied in biomedical materials and environmental friendship.^{12–15} In this direction, poly(vinyl alcohol) (PVA) is one of the most promising polymers, which is a water-soluble and biodegradable semi-crystalline polymer with good thermal stability, biocompatibility, nontoxicity, and chemical resistance.¹⁶ Therefore, they can be used widely such as membrane, cosmetic, adhesive and pharmaceutical materials, and so on.^{16–18} In the previous reports, there are many researches on PVA fibers produced by electrospinning technique. Ultrafine PVA fibers are considered as potential application materials in filtration and biomedical engineering, and so on.^{19–21}

Incorporating nanoparticles into the polymer is an effective method for enhancing the mechanical properties and thermal stabilities of polymeric nanofiber. On the other hand, polymer/layered crystal nanocomposites have been reported in a few studies. Some of the polymers such as polycaprolactone, poly-(lactic acid), and Nylon 6 have been used for

Correspondence to: Y. Liu (yua_liu@163.com).

Contract grant sponsor: The National Natural Science Foundation of China; contract grant number: 51073106.

the preparation of nanocomposite fibrous mats.^{1,13,14} Utilizing inorganic particles to enhance the mechanical and thermal properties of polymers has been studied. For example, Hyun reported that adding 5.0 wt % layered silicate (montmorillonite) to PVA could bring to an increment of 25% in tensile stress (TS) rate.²² Among the numerous inorganic materials, layered double hydroxide (LDH), known as a host-guest material, is constituted by positively charged hydroxide layers with intercalating anions and water molecules. Typically, the composition of LDH can be represented by the ideal formula $[M_{1-x}^{2+}M_x^{3+}(\text{OH})_2]^{x+}A_{x/n}^{n-}\cdot m\text{H}_2\text{O}$, where M^{2+} and M^{3+} are divalent and trivalent metal cations within the host layers of hydroxide sheets, such as Zn^{2+} or Al^{3+} , and A^{n-} is an interlayer anion, such as NO_3^- , CO_3^{2-} , or SO_4^{2-} .^{23,24} LDHs are considered as important layered crystals because of their wide range of practical applications in catalysis, flame retardants, photochemistry, and electrochemistry, and so on.²⁵ More recently, because of their abilities to intercalate anionic drugs, biocompatibility, and variable chemical composition, LDHs are also used in medicine, such as in antacid agents, antipepsin agents, and pharmaceutical formulations.²⁶ As the LDHs possess strong electrostatic interactions between adjacent layers, well dispersion of LDHs in water or other non-aqueous solvents is very difficult to obtain. To achieve a good dispersion of LDHs into polymer matrix, there have been many reports on intercalating a wide diversity of organic or inorganic anions to modify the properties of the LDH and improve the compatibility with the solvents.²⁷⁻²⁹

In this study, fibrous mat of PVA/LDH composites with good mechanical properties is prepared via electrospinning. Lactate anions are intercalated into the Mg-Al-layered double hydroxide (LDH) to improve the hydrophilicity of the LDH and the compatibility with PVA. The structure, morphology, and thermal property of the PVA/LDH nanofibrous mats are investigated by using Fourier transform infrared (FTIR), X-ray diffraction (XRD), scanning electron microscopy (SEM), transmission electron microscopy (TEM), thermogravimetric analysis (TGA), and mechanical measurements.

EXPERIMENTAL

Materials

$\text{Mg}(\text{NO}_3)_2\cdot 6\text{H}_2\text{O}$ and $\text{Al}(\text{NO}_3)_3\cdot 9\text{H}_2\text{O}$ were purchased from Kelong Chemical Reagent (Chengdu, China). Na_2CO_3 and NaOH were purchased from Changzheng Chemical Reagent (Chengdu, China). PVA (number-average degree of polymerization = 1700 and degree of saponification = 88%) was provided

by Sichuan Weinilun Industry (Chongqing, China) and was used after dried under vacuum at 50°C until constant weight.

Synthesis of the Mg/Al LDH- CO_3 and Mg/Al L-lactic acid-modified LDH

The LDH- CO_3 was prepared by coprecipitation method at constant pH value. Typically, a mixed aqueous solution of 50 mL of $\text{Mg}(\text{NO}_3)_2\cdot 6\text{H}_2\text{O}$ (0.075 mol) and $\text{Al}(\text{NO}_3)_3\cdot 9\text{H}_2\text{O}$ (0.025 mol) was mixed with 50 mL of Na_2CO_3 (0.05 mol) and NaOH (1 mol) aqueous solution by adding dropwise with vigorous stirring. To maintain the mixture at pH = 10.0, an aqueous solution of NaOH (2 mol L^{-1}) was titrated simultaneously, and the solution was vigorously stirred at 80°C for 12 h. The solid was centrifuged, washed several times with deionized water, and then was dried at room temperature.

The magnesium/aluminum LDHs containing lactate (Lact-LDH) was obtained according to a previously reported procedure.²⁸ The synthesis was carried out by coprecipitation. An aqueous solution of L-lactic acid was adjusted to pH 10 by adding NaOH solution, and then a mixed aqueous solution of $\text{Mg}(\text{NO}_3)_2\cdot 6\text{H}_2\text{O}$ (0.075 mol) and $\text{Al}(\text{NO}_3)_3\cdot 9\text{H}_2\text{O}$ (0.025 mol) was added dropwise. To maintain the mixture at pH = 10.0, an aqueous solution of NaOH (8 mol L^{-1}) was titrated simultaneously. The solution was vigorously stirred at room temperature for 24 h, whereas all synthetic procedures were carried out under nitrogen to minimize contamination from CO_2 in the air. The mixture was centrifuged, and washed several times with deionized water. The suspension of Lact-LDH was stored in water and took 3–5 days to become translucent.

Preparation of PVA/LDH blend solution

The PVA solution (8 wt %) was prepared by dissolving the polymers in doubly distilled water at 80°C under mechanical stirring for 5 h. Triton X-100, with concentration range of 0.1–0.2 v/w%, was added to the PVA solution. Triton X-100 surfactant was used to lower the surface tension of the polymer solution. Then different amounts of LDH- CO_3 or Lact-LDH were added to the solution and thoroughly mixed by ultrasonic waves to form a stable spinnable suspension.

ELECTROSPINNING OF PVA/LDH NANOFIBER MATS

The PVA/LDH nanofiber mats were prepared by electrospinning method. During electrospinning, solution of PVA/LDH was loaded into 10mL syringe with a stainless steel blunt-ended needle

with inner diameter of 0.8 mm. The solution was delivered to the needle via syringe pump at a constant flow rate (0.3 mL/h). A copper wire as the positive electrode was mounted in the spinneret and a grounded aluminum foil was used as the counter electrode which was located at a distance of 20 cm from the needle tip. A high voltage of 21 kV was applied to the PVA/LDH solution.

Characterizations

FTIR spectra

The FTIR spectra of the LDH-CO₃ and Lact-LDH materials were investigated using a Nicolet 6700 spectrophotometer over the wavenumber range of 400–4000 cm⁻¹. The powdered samples were mixed with KBr as 1 : 100 by mass.

Scanning Electron Microscopy

The morphology and properties characterization of the electrospun PVA, PVA/LDH-CO₃, and PVA/Lact-LDH fibers were examined by SEM using a JSM-5900LV electron microscope (JEOL, Japan) after applying gold coating.

Transmission Electron Microscopy

The dispersion of LDH-CO₃ and Lact-LDH in the PVA/LDH-CO₃ and PVA/Lact-LDH electrospun fibers was examined by TEM, respectively. Bright-field TEM images were recorded using a Hitachi H-600 instrument at an accelerating voltage of 75 kV.

XRD measurements

The XRD diffractograms of neat PVA and PVA/Lact-LDH fibers were examined by XRD measurements. The equipment was conducted on a Philips electronic instrument with Cu K α radiation in the range of $2\theta = 2\text{--}70^\circ$ at a scan rate of $2^\circ/\text{min}$, and was operated at 40 kV and 35 mA under room temperature.

Thermogravimetric analysis

Thermal analysis on neat PVA and PVA/LDH fibers was characterized on a NETZSCH TG 209 F1 under a nitrogen flow (50 mL min^{-1}) at a heating rate of $10^\circ\text{C min}^{-1}$ from 40 to 700°C .

Mechanical properties of the composite nanofibers

Mechanical property testing was performed by YG001A electronic fiber strength tester (Taicang Textile Instrument Factory). Strain rate was 20 mm min^{-1} and load cell was 150 CN. The samples were

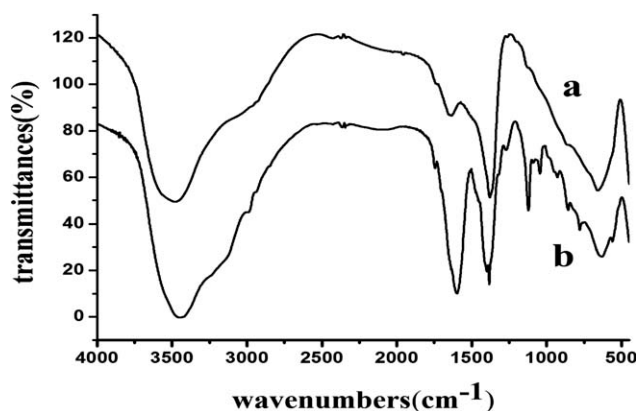


Figure 1 IR spectra of (a) LDH-CO₃ and (b) Lact-LDH.

prepared in $3\text{ mm} \times 20\text{ mm}$ (width and length) and their thicknesses were about $5\ \mu\text{m}$.

RESULTS AND DISCUSSION

Organic modification of Mg–Al–LDH

The FTIR spectra of the LDH-CO₃ and Lact-LDH samples are shown in Figure 1. A band around $3400\text{--}3500\text{ cm}^{-1}$ has been attributed to O–H stretching vibration of both the hydroxide basal layer and the interlayer water. The LDH-CO₃ and Lact-LDH samples show a band at 1376 cm^{-1} , which can be assigned to the asymmetric stretching vibration of the nitrate anions.³⁰ In Figure 1(b), the weak absorption peak of C–H antisymmetric stretches from the modes of the CH₃ group is observed in 2980 cm^{-1} region, and the strong absorption peak of C–O vibrations from the hydroxyl group that assigned to the lactate anion (CH₃-CHOH-COO⁻) in the Lact-LDH sample gives rise to absorptions in 1122 cm^{-1} , respectively. These peaks demonstrate that the lactate anion exists in the LDH.

Surface morphology of the LDH particles was investigated by SEM. As shown in Figure 2(b), the LDH-CO₃ is tightly coagulated owing to the high charge density of the layers and the high content of anionic species and water molecules, which result in strong interlayer electrostatic interactions between the sheets and the agglomeration.³¹ After being modified with the lactic acid, the Lact-LDH is crystallized into large-sized platelets [Fig. 2(a)], and therefore may have better dispersibility in water than that of LDH-CO₃.

Morphology of the neat PVA, PVA/LDH-CO₃, and PVA/Lact-LDH nanofibers

Optimizing condition for electrospinning processing, PVA concentration of 8%, and a distance from the needle tip to the grounded aluminum foil of 20 cm were applied. The morphologies of the obtained

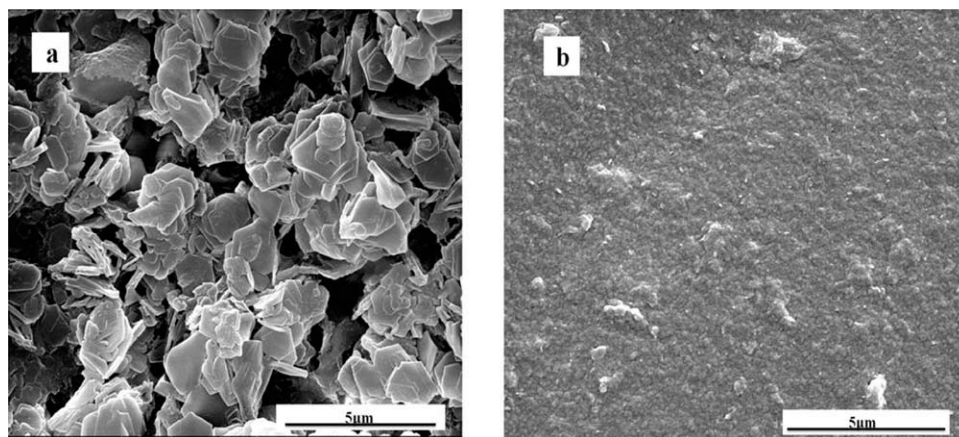


Figure 2 SEM micrograph of 3 : 1 LDH. (a) Lact-LDH and (b) LDH-CO₃. The magnification is 20,000× and scale bar is 5 μm.

nanofibers are shown in Figures 3 and 4. The PVA/LDH-CO₃ composite fibers [Fig. 3(a,c)] have a relative rough surface with some obvious knobs, whereas the PVA/Lact-LDH composite fibers [Fig. 3(b,d)] exhibit uniform, slick surface, and few knobs.

As shown in the SEM photographs with large amplification [Fig. 4(a)], the electrospun nanofibers of neat PVA have a diameter in the range of 400–500 nm. PVA/LDH-CO₃ composites with 3 and 5 wt % of nanoparticles are spun successfully, as shown in Figure 4(b,c). With increasing LDH-CO₃ contents, the agglomerated inorganic particles may occasion-

ally clog the needle during the electrospinning process, and the solution cannot be spun when incorporated 7 wt % of LDH-CO₃. It is difficult for the LDH-CO₃ to be homogeneously dispersed in polymer matrices. Therefore, it results in obvious agglomeration. Figure 5 shows the stability of the dispersion of neat PVA, PVA/LDH-CO₃, and PVA/Lact-LDH in aqueous solution after ultrasonication. Both LDH-CO₃ and Lact-LDH nanoparticles can disperse well in the PVA solution just after the ultrasonication. However, the LDH-CO₃ nanoparticles deposit at the bottom of the bottle after 1 h because of

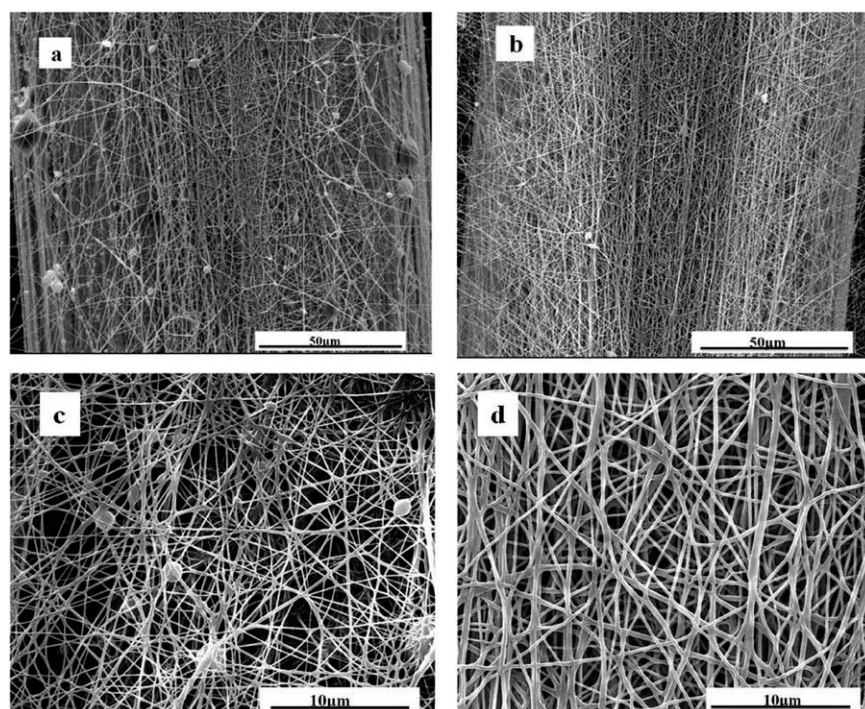


Figure 3 SEM micrographs of electrospun fibers (applied voltage, 20–21 kV; PVA solution concentration, 8 wt %). (a, c) PVA/3% LDH-CO₃, (b, d) PVA/3% Lact-LDH. (a, b) The magnification is 2000× and the scale is 50 μm; (c, d) the magnification is 10,000× and the scale is 10 μm.

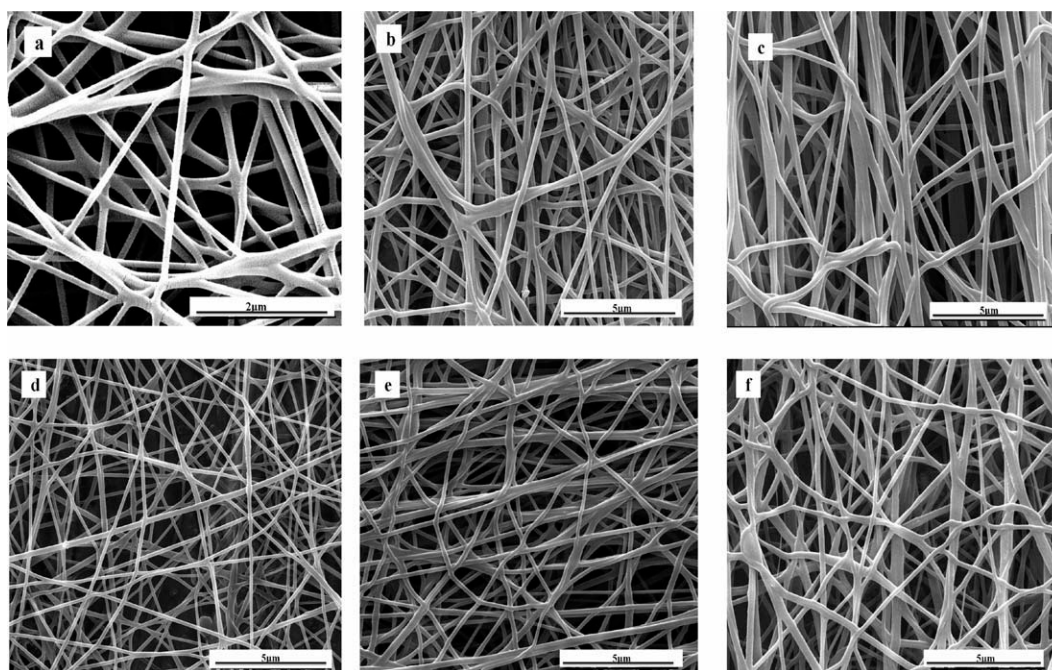


Figure 4 SEM micrographs of electrospun fibers (applied voltage, 20–21 kV; PVA solution concentration, 8 wt %). (a) Neat PVA, (b) PVA/3% LDH-CO₃, (c) PVA/5% LDH-CO₃, (d) PVA/3% Lact-LDH, (e) PVA/5% Lact-LDH, and (f) PVA/7% Lact-LDH. The magnification is 20,000× and the scale is 5 μm.

the agglomeration, whereas the Lact-LDH can keep stable even after a long time storing.

The dispersity of the nanoparticles plays an important role in determining the morphology of obtained nanofibers. As shown in the photographs of nanofibers of PVA/Lact-LDH with the 3, 5, and 7 wt % of Lact-LDH, the average diameters of PVA/Lact-LDH nanofibers are significantly lower (100–200 nm) compared with neat PVA or PVA/LDH-CO₃ fibers. After being modified with lactate, the PVA/Lact-LDH can form stable translucent colloidal solutions in water [Fig. 5(b)]. Therefore, the dispersion of Lact-LDH improves the electrospinnability of the mixture well, which results in a decrease in average diameter of fibers.¹

To investigate the dispersion of nanoparticles in the PVA nanofibers, the PVA/LDH-CO₃ and PVA/

Lact-LDH composite fibers are analyzed by the TEM images. Figure 6(a,b) shows the TEM micrographs of electrospun fibers of PVA/5% LDH-CO₃. Obvious aggregation of the nanoparticles is observed on the surface of the nanofibers, which suggests that the LDH in carbonate form have poor dispersibility in PVA matrix, and therefore results in much rougher and knobbed surface of fiber [Fig. 3(a,c)]. However, as shown in Figure 6(b,c), the Lact-LDH nanoparticles with content of 3 and 5% can be well dispersed in the inner of the electrospun PVA/Lact-LDH fibers with high degree of dispersion and uniformity. The lactic acid in the interlayer of LDH may weaken the strong cohesion between layers of the nanoparticles and interact with PVA chains, and therefore greatly improves the dispersibility of LDH in PVA matrix.

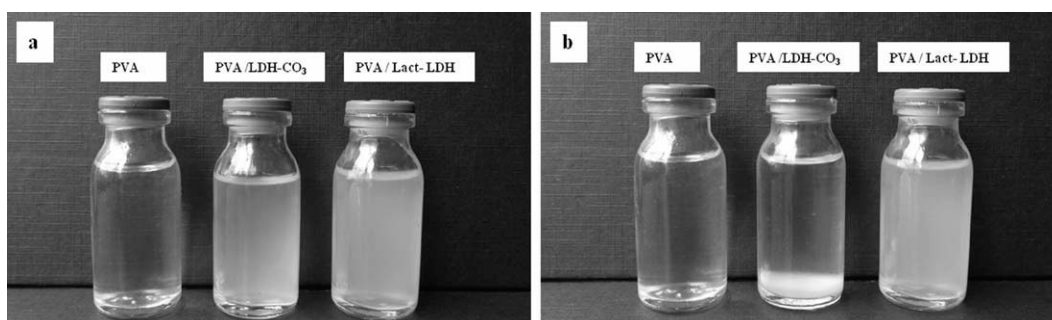


Figure 5 Images of the appearances of LDH dispersion in PVA solutions. (a) After ultrasonication, (b) after storage for 1 h.

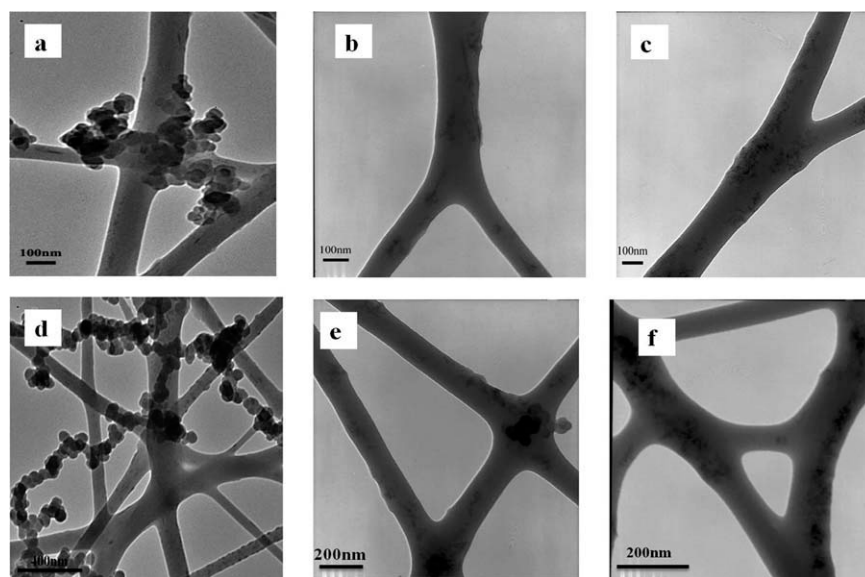


Figure 6 TEM images of electrospun fibers. (a, d) PVA/5% LDH-CO₃, (b, e) PVA/3% Lact-LDH; (c, f) PVA/5% Lact-LDH.

XRD diffractograms of the neat and composite samples

The XRD patterns in the range $2\theta = 2\text{--}70^\circ$ of neat PVA, PVA/3% Lact-LDH, PVA/5% Lact-LDH, and Lact-LDH are shown in Figure 7. From the XRD diffractograms of Lact-LDH, it is seen that the Lact-LDH has highly crystalline nature and layered geometry. A diffraction peak is observed at 2θ of 19.3° corresponding to the main peaks for the semi-crystalline PVA. For the composite fibers of PVA/Lact-LDH, diffraction peaks of the Lact-LDH, which increase with increasing content of Lact-LDH, are also observed.

Thermal properties of neat PVA, PVA/LDH-CO₃, and PVA/Lact-LDH Samples

The influence of LDH-CO₃ and Lact-LDH on thermal degradation of PVA was investigated by TGA.

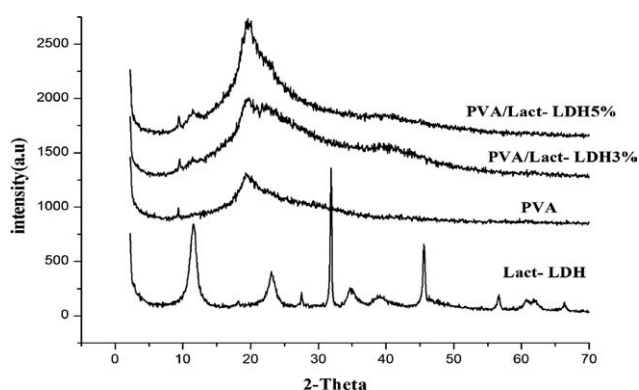


Figure 7 XRD diffractograms of neat PVA, PVA/Lact-LDH, and Lact-LDH.

The thermal degradation behaviors of neat PVA and nanocomposites with different contents of LDH-CO₃ and Lact-LDH in nitrogen atmosphere are shown in Figure 8 and Table I, respectively. As shown in Fig. 8, similar to that of neat PVA, there are two major weight loss stages for PVA/Lact-LDH and PVA/LDH-CO₃ nanocomposites. It appears that the introduction of nanoparticles decreases the onset temperature of degradation (T_{onset}). Moreover, as the addition of more LDH-CO₃ and Lact-LDH into PVA matrix, the T_{onset} continuously decreases. The result of decreased thermal stability is attributed to the catalysis of the Lact-LDH for the decomposition of PVA.^{31,32} Within up to 400°C, all nanocomposites exhibit enhanced thermal stability and a greater char yield compared to neat PVA. Besides, from the TGA curve in Figure 8 and Table I, it can be seen that the thermal stability of PVA/Lact-LDH nanocomposite is higher than that of PVA/LDH-CO₃ nanocomposite. The dispersibility of Lact-LDH nanoparticles in PVA solution is better than that of LDH-CO₃, which can be observed from the SEM micrographs [Fig. 3(a)] and TEM micrographs (Fig. 6). Therefore, the well-dispersed layered LDH particles may play a role of superior insulator, and therefore result in an improved thermal stability of PVA/Lact-LDH nanocomposite compared with PVA/LDH-CO₃ nanocomposite.³³

Mechanical properties

Mechanical durability of electrospun nanofibrous materials is important for their practical applications. The changes of the mechanical properties of

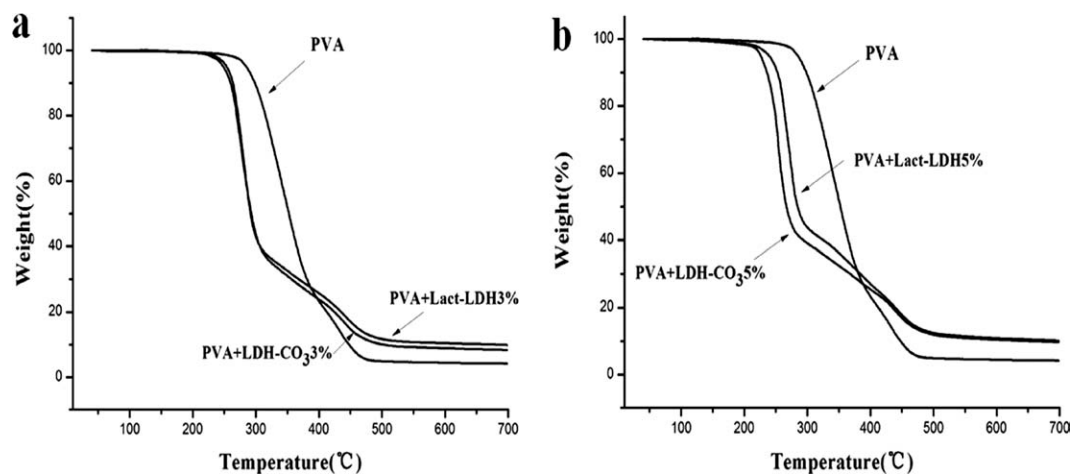


Figure 8 The thermal degradation of neat PVA and its hybrids with different amounts of LDH-CO₃ and Lact-LDH loadings in nitrogen atmosphere.

the PVA nanofibrous mats with or without LDHs were investigated. The variation of TS and elongation at break (EB) for PVA, PVA/LDH-CO₃, and PVA/Lact-LDH nanocomposites is summarized in Table II. The TS and EB of electrospun PVA/Lact-LDH fibrous mats are significantly higher than those of neat PVA nanofibers (TS is 10.4 MPa, and EB is 18.5%). The TS and EB of the nanofibrous mat increase with increasing Lact-LDH content in nanocomposite and are maxima with the 5 wt % Lact-LDH loading. This increase of TS and EB is owing to high degree of dispersion and uniformity between the polymer matrix and the inorganic nanoparticles. However, it is found that the TS and EB of PVA/Lact-LDH fibrous mats with 7 wt % Lact-LDH content are decreased. This is owing to the increasing tendency of agglomeration and the platelet orientation of Lact-LDH particles in the PVA matrix. It also appears that the TS and EB for PVA/LDH-CO₃ nanocomposite are improved compared to those of neat PVA. The maximum TS and EB (TS is 13.8

MPa, and EB is 27.8%) are observed for PVA/LDH-CO₃ nanocomposite with the 3 wt % LDH-CO₃ loading. However, the degree of increment in TS and EB of electrospun PVA/LDH-CO₃ fibrous mats is lower than that of PVA/Lact-LDH fibrous mats. This is attributed to the obvious agglomeration of LDH-CO₃ in the PVA matrix.

CONCLUSIONS

In summary, the nanofibers of PVA/LDH composites are successfully prepared by the electrospinning method in aqueous solutions. The morphological analysis shows that the diameter of PVA/Lact-LDH nanofibers is decreased compared to that of the neat PVA, indicating improved electrospinnability of PVA. The TEM investigations show that the dispersity of the LDH in PVA matrix is much improved after modification with L-lactic acid. The dispersity of LDH nanoparticles in PVA matrix plays an important role for mechanical properties of the composites fibrous mats. Modification of LDH with lactic acid obviously increases the dispersity of LDH, and therefore improves the mechanical properties of the fibrous mat comparing to those of neat PVA and PVA/LDH-CO₃ composites.

TABLE I
Thermal Properties of Electrospun Neat PVA, PVA/LDH-CO₃, and PVA/Lact-LDH Fibers^a

Sample	T_{onset} (°C)	T_{max1}	T_{max2}	Char residue (%) (700°C)
Neat PVA	284.8	348.2	436.1	4.23
PVA/3%LDH-CO ₃	248.6	276.6	440.3	8.36
PVA/3%Lact-LDH	253.6	283.6	440.9	9.87
PVA/5%LDH-CO ₃	226.0	253.5	440.6	9.65
PVA/5%Lact-LDH	239.1	272.7	436.6	10.14

^a T_{onset} , temperature at which 5% degradation occurs; T_{max1} and T_{max2} , temperatures obtained from DTG curves at which the maximum mass loss rate occurs during the first and second steps; Char, the fraction of the residue remaining at 700°C.

TABLE II
Tensile Properties of Neat PVA, PVA/Lact-LDH, and PVA/LDH-CO₃

Sample	TS (MPa)	EB (%)
Pure PVA	10.4 ± 0.88	18.6 ± 1.89
PVA/3%Lact-LDH	24.1 ± 1.05	34.4 ± 1.83
PVA/5%Lact-LDH	31.7 ± 0.71	36.6 ± 2.96
PVA/7%Lact-LDH	26.8 ± 0.61	27.8 ± 1.55
PVA/3%LDH-CO ₃	17.6 ± 1.18	24.4 ± 2.66
PVA/5%LDH-CO ₃	13.8 ± 1.17	22.0 ± 2.41

References

1. Valentina, R.; Giuliana, G.; Vittoria, V. *Biomacromolecules* 2007, 8, 3147.
2. Jamil, A. M.; Gary, E. W.; David, G. S.; Gary, L. B. *Biomacromolecules* 2002, 3, 232.
3. Deitzel, J. M.; Kosik, W.; McKnight, S. H. *Polymer* 2002, 43, 1025.
4. Liu, H. Q.; Hsihe, Y. L. *J Polym Sci Part B: Polym Phys* 2002, 40, 2119.
5. Theron, S. A.; Zussman, E.; Yarin, L. *Polymer* 2004, 45, 2017.
6. Chen, L. S.; Huang, Z. M.; Dong, G. H. *Polym Compos* 2009, 30, 239.
7. Huang, Z. M.; Zhang, Y. Z.; Ramakrishna, S.; Lim, C. T. *Polymer* 2004, 45, 5361.
8. Homaeigohara, S. S.; Buhra, K.; Ebert, K. *J Membr Sci* 2010, 365, 68.
9. Faheem, A. S.; Nasser, A. M. B.; Muzafar, A. K. *J Appl Polym Sci* 2010, 115, 3189.
10. Wang, S. C.; Zhang, B.; Sun, Z. Y. *Mater Lett* 2010, 64, 9.
11. Kyunghwan, Y.; Kwangsok, K.; Wang, X. F. *Polymer* 2006, 47, 2434.
12. Kim, Y. J.; Ahn, C. H. *Eur Polym J* 2010, 46, 1957.
13. Zhao, N. Q.; Shi, S. X.; Lu, G.; Wei, M. *J Phys Chem Solid* 2008, 69, 1564.
14. Fong, H.; Liu, W. D.; Wang, C. S. *Polymer* 2002, 43, 775.
15. Liu, F. J.; Guo, R.; Shen, M. W.; Wang, S. Y. *Macromol Mater Eng* 2009, 294, 666.
16. Krumova, M.; Lopez, D.; Benavente, R.; Mijangos, C.; Perena, J. M. *Polymer* 2000, 41, 9265.
17. Yang, J. H.; Yoon, N. S.; Jae, H. P.; Kim, I. K. *J Appl Polym Sci* 2011, 120, 2337.
18. Shao, C. G.; Kimb, H. Y.; Gong, J.; Ding, B. *Mater Lett* 2003, 57, 1579.
19. Wang, S. H.; Sun, L. G.; Zhang, B.; Wang, C. *Polym Compos* 2011, 32, 519.
20. Islam, M. S.; Karim, M. R. *Colloids Surf A: Physicochem Eng Aspects* 2010, 366, 135.
21. Hang, A. T.; Beomseok, T.; Park, J. S. *Carbohydr Polym* 2010, 82, 472.
22. Hyun, W. L.; Mohammad, R. K.; Hyun, M. J. *J Appl Polym Sci* 2009, 113, 1860.
23. Yang, J. T.; Chen, F.; Ye, Y. C. *Colloid Polym Sci* 2010, 288, 761.
24. Costa, F. R.; Satapathy, B. K.; Wagenknecht, U. *Eur Polym J* 2006, 42, 2140.
25. Dagnon, K. L.; Chen, H. H. *Polym Int* 2009, 58, 133.
26. Li, F.; Duan, X. *Struct Bonding* 2006, 119, 193.
27. Hibino, T. *Chem Mater* 2004, 16, 5482.
28. Hibino, T.; Kobayashi, M. *Chem Mater* 2005, 15, 653.
29. Jaubertie, C.; Holgado, M. J.; San Roman, M. S.; Rives, V. *Chem Mater* 2006, 18, 3114.
30. Eili, M.; Wan, M. Z. W. Y.; Zobir, H.; Mansor, A.; Nor, A. I. *J Appl Polym Sci* 2010, 118, 1077.
31. Zvonimir, M.; Marko, R.; Juraj, S. *Polym Degrad Stab* 2009, 94, 95.
32. Chiang, M. F.; Wu, T. M. *Compos Sci Technol* 2010, 70, 110.
33. Ding, Y. Y.; Gui, Z. *Mater Res Bull* 2008, 43, 212.